Photoacoustic Dual-mode Microsensor Based on PMUT Technology

Yiyun Wang [†]
Hybrid Imaging System Laboratory
School of Information Science and Technology
Shanghai Engineering Research Center of Energy Efficient and
Custom AI IC
ShanghaiTech University, Shanghai, China
wangyy@shanghaitech.edu.cn

Junxiang Cai [†]
School of Information Science and Technology,
Shanghai Engineering Research Center of Energy Efficient and
Custom AI IC,
ShanghaiTech University, Shanghai, China
Shanghai Institute of Microsystem and Information Technology,
Chinese Academy of Sciences, Shanghai, China
University of Chinese Academy of Sciences, Beijing, China
caijx1@shanghaitech.edu.cn

Tao Wu[*]
School of Information Science and Technology,
Shanghai Engineering Research Center of Energy Efficient and
Custom AI IC,
ShanghaiTech University, Shanghai, China
Shanghai Institute of Microsystem and Information Technology,
Chinese Academy of Sciences, Shanghai, China
University of Chinese Academy of Sciences, Beijing, China
wutao@shanghaitech.edu.cn

Fei Gao[*]
Hybrid Imaging System Laboratory
School of Information Science and Technology
Shanghai Engineering Research Center of Energy Efficient and
Custom AI IC
ShanghaiTech University, Shanghai, China
gaofei@shanghaitech.edu.cn

Abstract—**Photoacoustic sensing and imaging have emerged in the biomedical field and shown great potentials. Miniaturization and multi-functionality are in need for practical sensing scenarios. As a minimal and economical solution, micromachined ultrasound transducers can be implemented into the photoacoustic sensing system. In this work, we present a photoacoustic dual-mode microsensor based on PMUT technique. PMUT has its fundamental resonance and other high-order resonances. It displays high sensitivity for signal detection at the fundamental resonant frequency, and wide bandwidth at its high orders. Taking advantage of PMUT's frequency-domain characteristic, we propose a dual-mode photoacoustic sensing method from a single received signal. As the preliminary results are shown in the manuscript, such a dual-mode microsensor has the potential to provide biological indicators and healthcare monitoring.**

Keywords— photoacoustic sensing, micromachined ultrasound transducer, signal analysis, AlN PMUT array

I. INTRODUCTION

Over recent decades, photoacoustic (PA) sensing and imaging have been widely researched in the biomedical aspect [1]–[5]. With the advances in laser delivery and integration technologies, PA systems tend to be compact, portable, and affordable [6]–[10]. However, the conventional piezoelectric transducers are limited due to their bulky size and optical opaque [11], [12].

Nowadays, more and more microsensors for acoustic detection are implemented into photoacoustic systems [13]. The conventional bulk piezoelectric transducer is limited by its size and fabrication in the usage of endoscopy. Fortunately, microelectromechanical systems (MEMS) technology can

provide a solution to miniaturize the size of transducers for the applications of endoscopic PAI. Microsensors based on MEMS technology can be divided into two types: piezoelectric micromachined ultrasound transducers (PMUTs) and capacitive micromachined ultrasound transducers (CMUTs). CMUT has a high working bias voltage limitation, which may cause safety risks in *in vivo* biomedical imaging applications. On the contrary, PMUT is more flexible and safe in the *in vivo* applications because it is a passive device. According to the working modes, PMUT can be divided into two types: thickness extension mode (TEM) and flexural vibration mode (FVM). Compared with TEM PMUTs, FVM PMUTs are easily fabricated into arrays at a low cost, which is advantageous for achieving real-time imaging [14]. Additionally, FVM PMUT has a much larger capacitance and lower electrical impedance, making it more robust against parasitic effects and better matched to the readout electronics [15].

FVM-mode PMUT has multiple resonance modes with various center frequencies, according to the solution in the form of Bessel function of the Helmhotz equation for the fixed membrane [16]. Traditionally, the fundamental resonance of PMUT has been widely utilized, whether it is used as a sensor or as an actuator [15], [17]–[20]. At the fundamental resonance frequency, PMUT has the highest sensitivity. However, the photoacoustic signal detected at the fundamental frequency of FVM PMUT has a long oscillation due to its low center frequency and narrow bandwidth [21]. Compared with fundamental resonance, the sensitivity at other high-order resonance is relatively low, but the corresponding -3dB bandwidth becomes much broader. These resonance modes are not fully utilized in previous studies. In this work, we take both types of resonance modes into account for better performance.

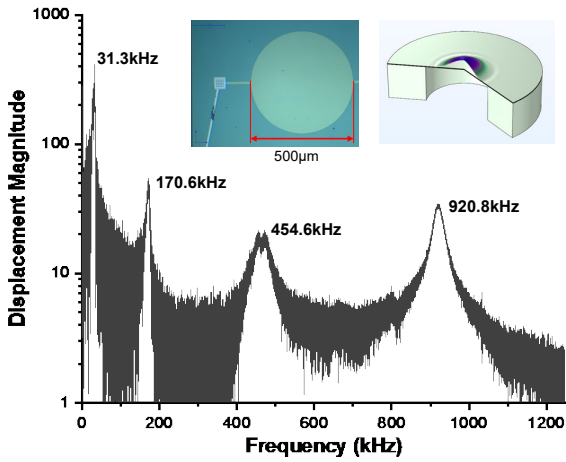Thus, based on PMUT's characteristic in the frequency domain, on the one hand, the frequency band with broad

Fig. 1. The LDV measurement of the PMUT array in mineral oil, the optical image and vibration mode of PMUT.

bandwidth yields high axial imaging resolution, which can be implemented to image the area of interest and locate the specific point of interest. It also shows the sensor's potential in frequency-domain analysis with tissue's properties, such as viscosity and elasticity [22]–[25]. On the other hand, the narrowband with large magnitude brings high sensitivity to the sensing applications, which may provide a long-term wearable monitoring device of key physiological parameters.

In this work, we report a PA dual-mode microsensor based on the PMUT technology. We use the fundamental resonance frequency of PMUT to get PA signal with high signal-to-noise ratio, and use other high-order resonance frequencies to obtain broadband PA signals with less oscillation, which can render higher resolution in imaging applications.

II. PMUT FABRICATION AND ANALYSIS

A. PMUT Design

A flexural vibration mode PMUT was designed and fabricated for photoacoustic dual-mode image [15-16]. As shown in Fig. 1, the cell's diameter is about 500 µm (effective working area). The PMUT is working in the mineral oil, in which the acoustic impedance is close to interstitial fluid. The frequency response of PMUT is measured by laser doppler velocimetry (LDV) in the mineral oil, which is shown as the curve of Fig. 1. It shows four resonance frequencies (center frequency), which are 31.1 kHz, 170.6 kHz, 454.6 kHz, and 920.8 kHz, respectively. The displacement magnitude of the fundamental frequency (the first-order frequency resonance mode) is significantly larger than that of other high-order resonance frequencies. However, the -3dB bandwidth of the first-order frequency is the narrowest in the four resonance frequency bands. FVM PMUT has more high-order resonance frequencies, but not shown in Fig. 1. The first four resonances are mainly analyzed in the demonstration of miniature wireless photoacoustic sensors.

B. Analysis of equivalent circuit model

In order to facilitate the analysis of energy transfer, the lumped element modeling (LEM) is widely used to analyze the responses of PMUTs [14], [26], [27]. Fig. 2(a) shows the LEM circuit of FVM PMUT for ultrasonic applications. It contains the acoustical, mechanical, and electrical domains. In

the equivalent circuit model, the acoustic domain is coupled to the mechanical domain through the coefficient Φ_1, which is indicated by the transformer of Fig. 2(a). Also, the mechanical domain and electrical domain are coupled by the coefficient Φ_2. PMUT can work as both sensor and actuator. Therefore, the LEM circuit mode can represent an electrical input with an acoustic pressure output and a pressure input with an electrical output.
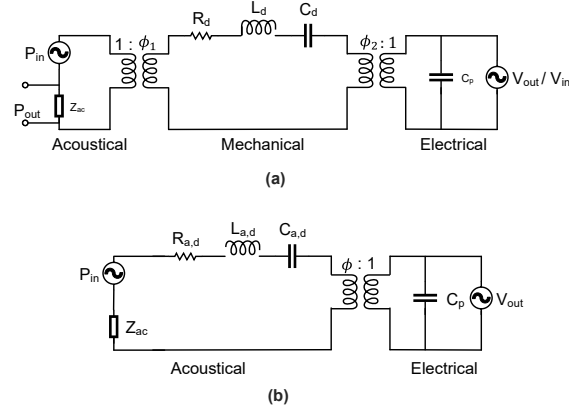

Fig. 2. (a). Lumped element modeling (LEM) circuit mode of a PMUT in three domains. (b). Simpilfed LEM circuit mode in two domains

In the LEM circuit model of Fig. 2(a), the lumped element Z_{ac} represents the acoustic radiation impedance of the membrane; C_d, R_d, and L_d are the mechanical compliance, mechanical damping, and effective mass of the membrane; and C_p is the measured electrical capacitance of the sandwiched piezoelectric element [28].

In PAI applications, PMUTs work as only acoustic sensors to receive photoacoustic signals. With known acoustical-mechanical coupling coefficient Φ_1, the LEM circuit mode can be simplified to Fig. 2(b). According to the new FEM elements, we can derive the critical parameters of FVM PMUT. The resonant frequency f_0:

$$f_0 = \frac{1}{2\pi}\sqrt{\frac{1}{L_{a,d}C_{a,d}}} \qquad (1)$$

And the quality factor Q can be expressed as:

$$Q = \frac{1}{R_{a,d} + \mathrm{Re}(Z_{ac})}\sqrt{\frac{L_{a,d}}{C_{a,d}}} \qquad (2)$$

By knowing f_0 and Q, we can easily derive the bandwidth of FVM PMUT:

$$\Delta f = \frac{f_0}{Q} = \frac{1}{2\pi}\frac{R_{a,d} + \mathrm{Re}Z_{ac}}{L_{a,d}} \qquad (3)$$

Each resonance of PMUT with different center frequency has a corresponding L_d, R_d, C_d. At the fundamental resonance, the sensor owns large displacement magnitude, which reflects its high sensitivity. The equivalent small R_d corresponds to a high quality factor, which indicates a narrow bandwidth. And other high-order resonances have a high equivalent R_d, which leads to a lower Q that leads to a broad frequency band and

less oscillation. The series resonance of L_d and C_d represents the resonance of PMUT.
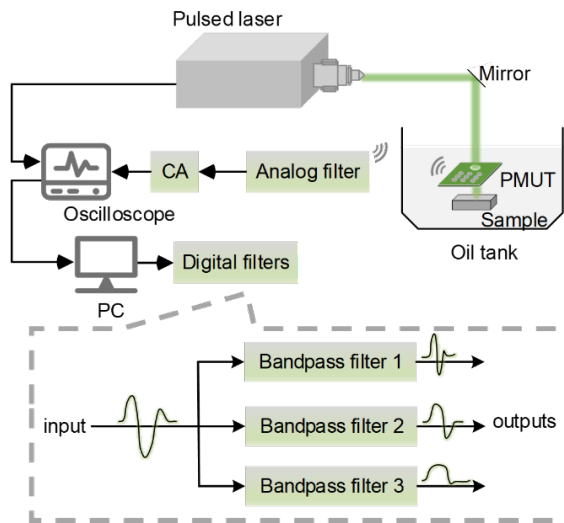

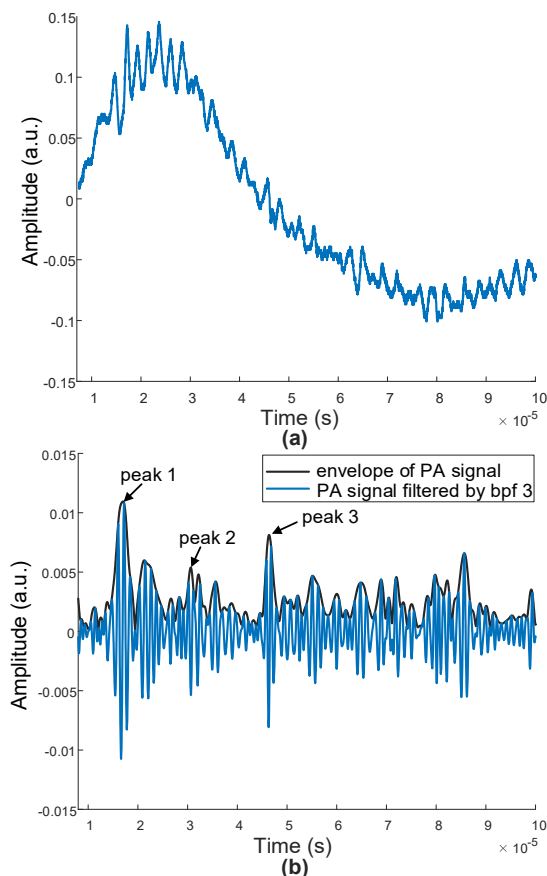Fig. 3. The diagram of the photoacoustic sensing system. PC: personal computer; CA: charge amplifier.

Fig. 4. (a). The original photoacoustic signal of a piece of green tape. (b). The selected PA signal through bandpass filter 3 and its envelope signal.

III. EXPERIMENTS AND RESULTS

Based on the design of the micromachined ultrasound transducer, we have conducted the experiments to present the feasibility of a dual-mode PA sensing with PMUT array.

A. Experiment Setup

The experimental setup is displayed in Fig. 3. A 532 nm pulsed laser (DPS-532-A, CNI Laser) generates laser illumination, traveling through the tiny hole on the PMUT's PCB board. The excited sample region absorbs the pulsed laser and emits ultrasound waves due to its thermal expansion. The ultrasound wave is then received by the PMUT array. After that, the PA signal passes through the analog high-pass filter to reduce low-frequency noise and is amplified through a charge amplifier. The preprocessed signal is displayed and averaged 14 times by the oscilloscope (DPO5204B, Tektronix Inc.) and collected by the personal computer.

Then, the PA signal goes through post-processing. According to PMUT's characteristic in the frequency domain, we have designed three digital band-pass filters; bandwidths are between 18 kHz and 100 kHz (bp filter 1), between 400 kHz and 700 kHz (bp filter 2), between 700 kHz and 1500 kHz (bp filter 3), respectively. In this way, the narrowband and broadband PA signals are generated from one single original signal.

B. Results and Analysis

We process the collected PA signals from the PMUT array in the following steps. Here, we set the PA signal excited by a piece of green tape on the glass slide as an example. The collected signal is pre-processed through the analog high-pass filter (Fig. 4(a)). It then passes through the selected digital filter, aiming at achieving the narrowband or broadband results. Finally, as shown in Fig. 4(b), the envelope waveform is extracted for analysis on the maximum PA magnitude and bandwidth. It is noticed that there are several peaks in Fig. 4(b). After comparing the actual distance and the distance that is converted by the peaks' interval, we identify peak 2 as the ultrasound signal from the back of the glass slide and peak 3 as the secondary ultrasonic echo from the tape. It indicates the microsensor's potential in discriminating tissues from different depths.
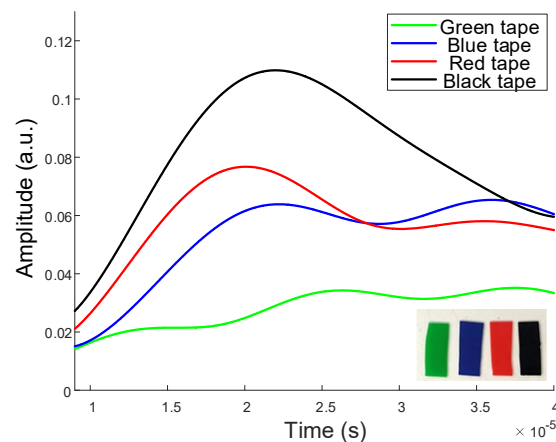

Fig. 5. The narrowband PA envelope signals excited from tapes in different colors. Inserted graph: Sample 1: a glass slide covered with tapes in green, blue, red, and black.

The first experiment is designed to verify the sensor's sensitivity in the narrow frequency band mode (bandpass filter 1). We conduct the experiment on sample 1, which is a piece of glass slide with tapes in different colors, shown in the inserted graph of Fig. 5. Due to the signals' oscillations, we focus on the first peaks of the envelope PA signals. As shown in Fig. 5, the amplitudes of these peaks ascend with their optical absorption from 532 nm pulsed laser. Tapes in different colors have their individual and unique optical absorptions. Thus, we may observe the PA signals with various dominant frequencies from the waveforms. The results indicate that the PMUT can discriminate samples of different optical absorptance with high sensitivity.
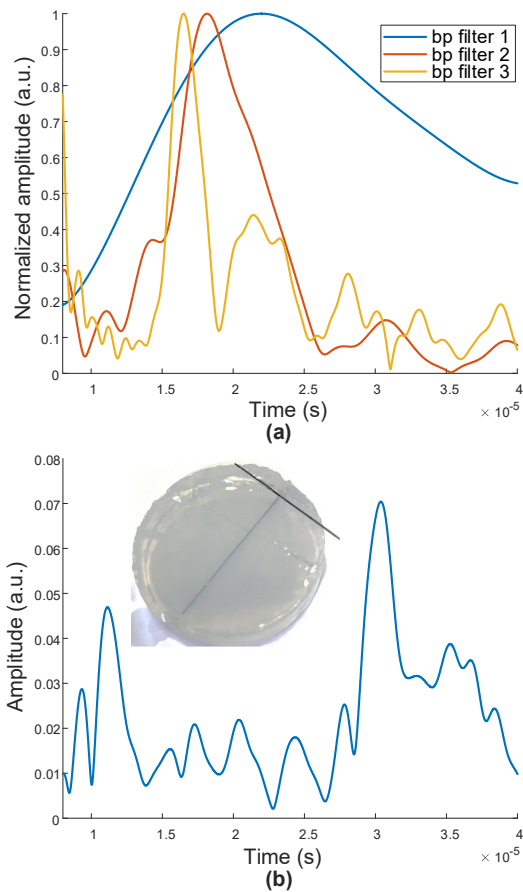

(a)

(b)

Fig. 6. (a). The amplitudes of normalized PA envelope signals through bandpass filter 1, 2, and 3. (b). The amplitude of the photoacoustic envelope signal (through bandpass filter 3) excited from the intersection point of two leads in the vertical view. Inserted graph: Sample 2 - an agar phantom with two pencil leads in parallel.

The second experiment shows PMUT's performance of high resolution in depth with the broadband mode. We present results through one narrowband filter and two broadband filters (Fig. 6(a)). The PA signals' full width at half maximum are 28.11 μs, 6.71 μs, and 2.63 μs, respectively. They descend with the resonance frequency increasing, which fits the theoretical analysis. The frequency band with a relatively high bandwidth is selected for further performance analysis of the microsensor. We fabricated an agar phantom with two parallel pencil leads placed on the top and bottom (the inserted graph in Fig. 6(b)). When the laser illuminates on the pencil leads' intersection on sample 2, PMUT receives the

broadband PA signal with two prominent peaks after being filtered by bandpass filter 3. The result qualitatively shows the microsensor's ability to provide sample depth information in the certain broadband mode. We will further research on extracting the depth information more precisely and quantitatively.

IV. CONCLUSION

In this work, the PA dual-mode PMUT sensing method is proposed, which shows high displacement magnitude at the fundamental resonance frequency and relatively broad bandwidth at other resonance frequencies. We take advantage of the PMUT's frequency-domain characteristics and implement them into the qualitative analysis of PA signals. The narrowband and broadband filters are designed based on PMUT's resonance frequencies. Through filtering, the original PA signals are analyzed with dual modes: high-sensitivity and high depth resolution modes. The experiments with tape samples and phantom sample validate its feasibility. The results show the PMUT ability to provide high-sensitivity and depth-related information at the same time. With the wireless transmission module, the proposed microsensor has the prospect of achieving a long-term wearable system for healthcare monitoring.

REFERENCES

[1] L. V. Wang, "Tutorial on photoacoustic microscopy and computed tomography," *IEEE J. Sel. Top. Quantum Electron.*, vol. 14, no. 1, pp. 171–179, 2008, doi: 10.1109/JSTQE.2007.913398.

[2] X. L. Deán-Ben and D. Razansky, "Optoacoustic image formation approaches - A clinical perspective," *Phys. Med. Biol.*, vol. 64, no. 18, 2019, doi: 10.1088/1361-6560/ab3522.

[3] H. Wu *et al.*, "Non-invasive monitoring of circulating melanoma cells by in vivo photoacoustic flow cytometry," 2019, no. March 2019, p. 13. doi: 10.1117/12.2507807.

[4] S. Jeon, J. Kim, D. Lee, J. W. Baik, and C. Kim, "Review on practical photoacoustic microscopy," *Photoacoustics*, vol. 15, no. July, p. 100141, 2019, doi: 10.1016/j.pacs.2019.100141.

[5] A. B. E. Attia *et al.*, "A review of clinical photoacoustic imaging: Current and future trends," *Photoacoustics*, vol. 16, p. 100144, 2019.

[6] E. Hysi, M. J. Moore, E. M. Strohm, and M. C. Kolios, "A tutorial in photoacoustic microscopy and tomography signal processing methods," *J. Appl. Phys.*, vol. 129, no. 14, 2021, doi: 10.1063/5.0040783.

[7] H. Zhong, D. Jiang, T. Duan, H. Lan, J. Zhang, and F. Gao, "Fingertip laser diode system enables both time-domain and frequency-domain photoacoustic imaging," *Proc. - IEEE Int. Symp. Circuits Syst.*, vol. 2019-May, no. 8, pp. 1988–1991, 2019, doi: 10.1109/ISCAS.2019.8702204.

[8] D. Jiang, H. Lan, Y. Xu, Y. Wang, F. Gao, and F. Gao, "Size-adjustable photoacoustic tomography system with sectorial ultrasonic transducer array," *Proc. - IEEE Int. Symp. Circuits Syst.*, vol. 2021-May, 2021, doi: 10.1109/ISCAS51556.2021.9401101.

[9] R. Zhang, K. Tang, C. Yang, H. Jin, S. Liu, and Y. Zheng, "Portable photoacoustic sensor for noninvasive glucose monitoring," *Proc. - IEEE Int. Symp. Circuits Syst.*, vol. 2019-May, pp. 1–4, 2019, doi: 10.1109/ISCAS.2019.8702322.

[10] H. Zhong and Y. Wang, "Multi-wavelengths Nonlinear Photoacoustic Imaging Based on Compact Laser Diode System," *2019 IEEE Biomed. Circuits Syst. Conf. BioCAS*, pp. 1–4, 2019.

[11] H. Wang, Y. Ma, H. Yang, H. Jiang, Y. Ding, and H. Xie, *Mems ultrasound transducers for endoscopic photoacoustic imaging applications*, vol. 11, no. 10. 2020. doi: 10.3390/mi11100928.

[12] D. Biqin, C. Sun, and H. F. Zhang, "Optical Detection of Ultrasound in Photoacoustic Imaging," *IEEE Trans. Biomed. Eng.*, vol. 64, no. 1, pp. 4–15, 2017, doi: 10.1109/TBME.2016.2605451.

[13] J. Li, B. E. F. De Ávila, W. Gao, L. Zhang, and J. Wang, "Micro/nanorobots for Biomedicine: Delivery, surgery, sensing, and detoxification," *Sci. Robot.*, vol. 2, no. 4, pp. 1–10, 2017, doi: 10.1126/scirobotics.aam6431.

[14] H. Wang, Y. Ma, H. Yang, H. Jiang, Y. Ding, and H. Xie, *Mems ultrasound transducers for endoscopic photoacoustic imaging applications*, vol. 11, no. 10. 2020. doi: 10.3390/mi11100928.

[15] Y. Qiu *et al.*, "Piezoelectric micromachined ultrasound transducer (PMUT) arrays for integrated sensing, actuation and imaging," *Sens. Switz.*, vol. 15, no. 4, pp. 8020–8041, 2015, doi: 10.3390/s150408020.

[16] L. E. Kinsler, A. R. Frey, A. B. Coppens, and J. V. Sanders, *Fundamentals of acoustics*. John wiley & sons, 2000.

[17] W. Liao *et al.*, "Piezoelectric micromachined ultrasound tranducer array for photoacoustic imaging," *2013 Transducers Eurosensors XXVII 17th Int. Conf. Solid-State Sens. Actuators Microsyst. TRANSDUCERS EUROSENSORS 2013*, no. June, pp. 1831–1834, 2013, doi: 10.1109/Transducers.2013.6627146.

[18] A. Dangi *et al.*, "A Photoacoustic Imaging Device Using Piezoelectric Micromachined Ultrasound Transducers (PMUTs)," *IEEE Trans. Ultrason. Ferroelectr. Freq. Control*, vol. 67, no. 4, pp. 801–809, 2020, doi: 10.1109/TUFFC.2019.2956463.

[19] H. Wang, P. X. L. Feng, and H. Xie, "A High-Density and Dual-Frequency PMUT Array Based on Thin Ceramic PZT for Endoscopic Photoacoustic Imaging," *Proc. IEEE Int. Conf. Micro Electro Mech. Syst. MEMS*, vol. 2021-Janua, no. January, pp. 891–894, 2021, doi: 10.1109/MEMS51782.2021.9375356.

[20] J. Cai, K. Liu, L. Lou, S. Zhang, Y. A. Gu, and T. Wu, "Increasing Ranging Accuracy of Aluminum Nitride Pmuts by Circuit Coupling," in *2021 IEEE 34th International Conference on Micro Electro Mechanical Systems (MEMS)*, Jan. 2021, pp. 740–743.

[21] J. Cai, Y. Wang, L. Lou, S. Zhang, F. Gao, and T. Wu, "Photoacoustic and Ultrosound Dual-Modality Endoscopic Imaging based on Aln Pmut Array," presented at the 2022 IEEE 35th International Conference on Micro Electro Mechanical Systems (MEMS).

[22] Y. Wang *et al.*, "Frequency-domain Dual-contrast Photoacoustic Imaging with Chirp Modulation," *Annu. Int. Conf. IEEE Eng. Med. Biol. Soc. EMBC*, vol. 201210, pp. 1–4, 2020.

[23] F. Gao, X. Feng, and Y. Zheng, "Photoacoustic elastic oscillation and characterization," *Opt. Express*, vol. 23, no. 16, p. 20617, 2015, doi: 10.1364/oe.23.020617.

[24] C. Lou and D. Xing, "Photoacoustic measurement of liquid viscosity," *Appl. Phys. Lett.*, vol. 96, no. 21, 2010, doi: 10.1063/1.3435462.

[25] F. Gao, X. Feng, Y. Zheng, and C.-D. Ohl, "Photoacoustic resonance spectroscopy for biological tissue characterization," *J. Biomed. Opt.*, vol. 19, no. 6, p. 067006, 2014, doi: 10.1117/1.jbo.19.6.067006.

[26] R. J. Przybyla *et al.*, "In-air rangefinding with an aln piezoelectric micromachined ultrasound transducer," *IEEE Sens. J.*, vol. 11, no. 11, pp. 2690–2697, 2011.

[27] A. Dangi and R. Pratap, "System level modeling and design maps of PMUTs with residual stresses," *Sens. Actuators Phys.*, vol. 262, pp. 18–28, 2017.

[28] Y. Lu, A. Heidari, and D. A. Horsley, "A high fill-factor annular array of high frequency piezoelectric micromachined ultrasonic transducers," *J. Microelectromechanical Syst.*, vol. 24, no. 4, pp. 904–913, 2014.